Multi-task Neural Networks for QSAR Predictions

George E. Dahl gdahl@cs.toronto.edu Navdeep Jaitly ndjaitly@cs.toronto.edu

Ruslan Salakhutdinov rsalakhu@cs.toronto.edu

Department of Computer Science, University of Toronto, 6 King's College Rd, Toronto, Ontario M5S 3G4, Canada

Abstract

Although artificial neural networks have occasionally been used for Quantitative Structure-Activity/Property Relationship (QSAR/QSPR)studies in the past, the literature has of late been dominated by other machine learning techniques such as random forests. However, a variety of new neural net techniques along with successful applications in other domains have renewed interest in network approaches. In this work, inspired by the winning team's use of neural networks in a recent QSAR competition, we used an artificial neural network to learn a function that predicts activities of compounds for multiple assays at the same time. We conducted experiments leveraging recent methods for dealing with overfitting in neural networks as well as other tricks from the neural networks literature. We compared our methods to alternative methods reported to perform well on these tasks and found that our neural net methods provided superior performance.

1 Introduction

Quantitative Structure Analysis/Prediction Studies attempt to build mathematical models relating physical and chemical properties of compounds to their chemical structure. Such mathematical models could be used to inform pharmacological studies by providing an *in silico* metholodogy to test or rank new compounds for desired properties without actual wet lab experiments. Already QSAR studies are used extensively to predict pharmacokinetic properties such as ADME (absorption, distribution, metabolism and excretion) and toxicity. Improvements in these methods could provide numerous benefits to the drug development pipeline.

Learning QSAR models requires three main steps: generating a training set of measured properties of known compounds, encoding information about the chemical structure of the compounds, and building a mathematical model to predict measured properties from the encoded chemical structure. High throughput screening (HTS) studies are ideal for collecting training data — a few hundred to thousands of compounds are now tested routinely using HTS equipment against an assay of interest (which may be cellular or biochemical). Generating molecular descriptors from compound structures is also a well studied problem and various methods of encoding relevant information about compounds as vectors of numbers have been developed. These descriptors measure various physical, chemical, and toplogical properties of the compounds of interest. Once descriptors have been computed, machine learning and statistics supply the mathematical models used to make the predictions. The particular machine learning techniques used matter a great deal for the quality of QSAR predictions. In a QSAR competition sponsored by $Merck^1$, all competitors used the same descriptors and training data, but nevertheless our machine learning techniques (in particular deep neural network models related to the neural nets we describe in this paper) allowed the winning $team^2$ to achieve a relative accuracy improvement of approximately 15% over Merck's internal baseline.

Applying machine learning algorithms to QSAR has a rich history. Early work applying machine learning to QSAR tasks used linear regression models, but these were quickly supplanted by Bayesian neural networks [Ajay et al., 1998, Burden, 1999, Burden et al., 2000] and other approaches. Recently, random forests [Svetnik et al., 2003], projection pursuit, partial least squares and support vector machines [Du et al., 2008, Si et al., 2007] have also been applied successfully to this task. Each of these methods has different advantages and disadvantages (see Liu and Long [2009] for a recent review). Practitioners in the field have often been partial to methods that, in addition to making accurate predictions, allow for variable selection, so that users are able to assess whether chosen features are indeed useful from the viewpoint of an informed chemist, and to methods that allow for easy assessment of uncertainty from the models. Also important has been the issue of controlling overfitting, although this is a concern that is paramount not only to QSAR, but all domains where high-capacity machine learning models are applied to small data sets. Random forests have, thus far, been well-suited to these requirements since they do not readily overfit and since they provide a simple measure of variable importance. Bayesian neural networks are particularly suitable for assessing uncertainty about model predictions and controlling overfitting. However, the computational demands of Bayesian neural networks necessitate small hidden layers and using variable selection to reduce the input dimensionality. Gaussian process regression models can be viewed as an infinite hidden layer limit of Bayesian neural networks, but can still be quite computationally expensive, often requiring time cubic in the number of training cases [Obrezanova et al., 2007].

¹http://www.kaggle.com/c/MerckActivity (Retrieved June 6, 2014)

²http://blog.kaggle.com/2012/11/01/deep-learning-how-i-did-it-merck-1st-place-interview/ (Retrieved June 6, 2014)

Non-Bayesian neural networks have also been applied to QSAR [Devillers, 1996], but often had only a single small hidden layer (presumably to avoid overfitting issues that Bayesian versions obviate). The past decade has seen tremendous improvements in training methods for deep and wide neural networks as well as a renewed appreciation for the advantages of deeper networks. Deep neural networks (DNNs) have been highly successful on a variety of different tasks including speech recognition [Hinton et al., 2012a], computer vision [Krizhevsky et al., 2012], and natural language processing [Collobert and Weston, 2008]. The methodological improvements, along with faster machines, have allowed researchers to train much larger and more powerful models — instead of neural networks with only one hidden layer with 20-50 hidden units, neural networks are now regularly trained with many hidden layers of thousands of hidden units, resulting in millions of tunable parameters. Networks this large can even be trained on small datasets without substantial overfitting using early stopping, weight penalties, and the newer techniques of unsupervised pre-training [Hinton et al., 2006] and dropout [Hinton et al., 2012b]. All of these techniques for avoiding overfitting in large neural nets trained on small datasets are relatively inexpensive computationally, especially compared to a fully Bayesian approach.

As mentioned above, the neural net QSAR models we trained in this work differ from those used in the QSAR literature in a variety of respects. However, the most important difference is that the neural nets we explore in this paper are multi-task neural networks that operate on multiple assays simultaneously, something that is very rare in the literature. The only other work we are aware of to use multi-task neural nets for QSAR is Erhan et al. [2006] and there are a variety of differences between it and the work we present here. In particular, we used the recently developed dropout technique to control overfitting and we did not have access to target protein features. Additionally, Erhan et al. [2006] focussed on exploring the performance of the kernel-based JRank algorithm for collaborative filtering and not different neural net variants.

The motivation behind multi-task learning is that performance on related tasks can be improved by learning shared models. Multi-task neural network models are particularly appealing because there can be a shared, learned feature extraction pipeline for multiple tasks. Not only can learning more general features produce better models, but weights in multi-task nets are also constrained by more data cases, sharing statistical strength. QSAR tasks naturally lend themselves to multi-tasking — assays are often related to each other and different compounds might share features. Even if assays are only tenuously related, they are still governed by the laws of chemistry and it might still be important to learn more broadly useful higher-level features from the initial descriptors.

In this paper, we apply multi-task learning to QSAR using various neural network models. We do this while leveraging some of the recent developments outlined above. Our results show that neural nets with multi-tasking can lead to significantly improved results over baselines generated with random forests.

2 Methods

The machine learning model that we use as the basis for our approach to QSAR is the feedforward (artificial) neural network (ANN). Neural networks are powerful non-linear models for classification, regression, or dimensionality reduction. A neural network maps input vectors to output vectors with repeated compositions of simpler modules called layers. The internal layers re-represent the input and learn features of the input useful for the task.

Mathematically, an *L*-layer neural network is a vector valued function of input vectors \vec{x} , parameterized by weight matrices \mathbf{W}_l and bias vectors \vec{b}_l , defined by:

$$\begin{split} \vec{y}_0 &= \vec{x} \\ \vec{z}_l &= \mathbf{W}_l \vec{y}_{l-1} + \vec{b}_l \\ \vec{y}_l &= h_l(\vec{z}_l), \end{split}$$

where the h_l are elementwise, nonlinear activation functions (such as $\frac{1}{1+e^{-x}}$), \vec{y}_l is the activation of layer l and \vec{z}_l is the net input to layer l. Given a dataset of known input and output vectors $\{(\vec{x}_n, \vec{t}_n)\}$, we optimize the parameters $\Theta = (\{\mathbf{W}_l\}, \{\vec{b}_l\})$ of the network to minimize some cost function. For standard regression problems, the output $\vec{y}(\vec{x}) = \vec{y}_L(\vec{x}_n; \Theta)$ and target vectors will be one dimensional. A typical cost function for regression is the mean squared error:

$$C_{MSE}(\Theta) = \frac{1}{2} \sum_{n=1}^{N} \|\vec{y}_L(\vec{x}_n; \Theta) - \vec{t}_n\|^2.$$

For classification problems, the cross-entropy error function is more appropriate. In the binary classification case, the cross entropy error is:

$$C_{CE}(\Theta) = -\sum_{n=1}^{N} t_n \log y(\vec{x}_n; \Theta) + (1 - t_n) \log(1 - y(\vec{x}_n; \Theta)).$$

We trained all neural networks in this work using minibatched stochastic gradient descent (SGD) with momentum. In other words, we repeatedly estimated $\frac{\partial C(\Theta)}{\partial \Theta}$ from a small minibatch of training cases and used it to update the "velocity" of the parameters (see the appendix A for details on the update rule).

2.1 Multi-task neural networks

The most direct application of neural networks to QSAR modeling is to train a neural net on data from a single assay using vectors of molecular descriptors as input and recorded activities as training labels. This single-task neural net approach, although simple, depends on having sufficient training data in a single assay to fit the model well. We suspect data scarcity is one reason agressively regularized models such as random forests are popular in the literature [Svetnik et al., 2003]. In order to leverage data from multiple assays, we use a multi-task neural net QSAR architecture that makes predictions for multiple assays simultaneously. Vectors of descriptors still serve as the input to the network, but there is a separate output unit for each assay. For any given compound, we typically only observe one or at most a small number of output values since in general we do not expect compounds to appear in all assays regularly. During multi-task neural net training we only perform backpropagation through output layer weights incident on output units whose value we observe for the current training case. For simplicity we treat a compound that appears in k different assays as k different training cases that have the same descriptor vector but different outputs observed. Since the number of compounds screened varies across assays, naïvely combining all the training cases from all the available assays and training a multitask neural net would bias the objective function towards whatever assay had the most compounds. We handle this issue by controlling how many training cases from each assay go into a minibatch. For example, if there are 7 assays we could create minibatches of 80 cases by drawing 20 cases at random (with replacement) from a particular assay we wish to emphasize and 10 cases from each of the other six assays.

Martin et al. [2011] presented another way of leveraging related assays called Profile-QSAR that is similar in spirit to the multi-task neural net approach we use (although it does not use neural nets), but has many important differences. Profile-QSAR treats some of the assays as side information and uses single task methods to complete an assay/compound activity matrix for these previously studied assays. The imputed and measured activities for a particular compound in the side information assays become additional descriptors to use when making predictions for the compound. Unlike Profile-QSAR, the multi-task neural net approach does not do any imputation of activities. Another difference is that a multi-task neural net trains on all available assays and potentially makes predictions on all available assays as well while learning a shared feature extraction pipeline.

2.2 Wider and deeper neural networks

Deep neural networks, or neural networks with multiple hidden layers, have been highly successful recently in numerous applications (notably computer vision [Krizhevsky et al., 2012] and speech recognition [Hinton et al., 2012a]) because they are capable of learning complicated, rapidly-varying non-linear functions and are also capable of extracting a hierarchy of useful features from their input. Many successful deep neural network models have millions of tunable parameters and wide layers with thousands of units. In contrast, neural nets used in QSAR to date tend to have only a single layer and sometimes very few hidden units (for example Lowe et al. [2012]). Recent advances in training and regularizing wide and deep neural nets and in computer hardware have changed the dominant approach to training neural networks in the machine learning community from training small nets that are incapable of overfitting and often underfit to instead agressively regularizing wide and deep neural networks with many tunable parameters. The most important lesson from the recent successes of deep learning is that, although deeper networks will not always perform better than shallow ones, practitioners need to be using models that can trade breadth for depth and vice versa, since one particular architecture cannot be the best for all problems. In this paper, we describe our initial attempts to leverage advances in deep neural network methods in QSAR applications. As assays become cheaper and more assay results accumulate, machine learning models with high capacity will have the best performance. Many of the models we trained (including nets with only a single hidden layer) have far more weights than we have training cases, but through careful training and regularization they can still perform well.

2.3 Regularizing large neural networks

Using wide and/or deep neural nets with many tunable parameters makes avoiding overfitting especially crucial. In QSAR modeling we often want to use large and expressive models capable of representing complex dependencies between descriptors and activities. but data may also be quite limited. Regularization, broadly construed, has been the subject of much recent deep learning research. Generative unsupervised pre-training [Hinton et al., 2006, Erhan et al., 2010] is a powerful data-dependent regularizer that brought a lot of attention to deep neural net models in particular. Early stopping of training based on validation error can partially control overfitting but has limited effectiveness when there is very little validation data and the networks being trained have very high capacity. Penalizing large weights in the model can also help avoid overfitting, although more sophisticated techniques are, in our experience, much more useful. One such technique is dropout [Hinton et al., 2012b]. Dropout randomly corrupts the activations of neurons in the network during training by zeroing out their activities independently. Intuitively, one effect the noise added by dropout has is that it penalizes large weights that result in uncertain predictions or hidden unit activations. Another way to view dropout is as approximate model averaging over the exponentially numerous different neural nets produced by deleting random subsets of hidden units and inputs. We can also view multi-task neural nets as a way of regularizing the weights that are shared across assays. Since only the output weights are assay-specific, using data from other assays is a powerful way of avoiding overfitting. Instead of shifting the weights towards zero the way an L2 penalty on the weights would, multi-task neural nets shift the weights of the hidden unit feature detectors towards values that extract features useful for other QSAR tasks. In this way, hidden layers in a multi-task neural network in-effect learn higher level, more abstract molecular descriptors and have a training objective that encourages them to create features useful for more than one task.

3 Experiments

In order to test the effectiveness of multi-task neural nets for QSAR we trained neural nets on publically available assay results and compared their performance to a selection of

AID	Assay Target / Goal	Assay Type	# active	# inactive
1851(2c19)	Cytochrome P450, family 2, subfamily C, polypeptide 19	Biochemical	5913	7532
1851(2d6)	Cytochrome P450, family 2, subfamily D, polypeptide 6,	Biochemical	2771	11139
. ,	isoform 2			
1851(3a4)	Cytochrome P450, family 3, subfamily A, polypeptide 4	Biochemical	5266	7751
1851(1a2)	Cytochrome P450, family 1, subfamily A, polypeptide 2	Biochemical	6000	7256
1851(2c9)	Cytochrome P450, family 2, subfamily C, polypeptide 9	Biochemical	4119	8782
1915	Group A Streptokinase Expression Inhibition	Cell	2219	1017
2358	Protein phosphatase 1, catalytic subunit, alpha isoform 3	Biochemical	1006	934
463213	Identify small molecule inhibitors of tim10-1 yeast	Cell	4141	3235
463215	Identify small molecule inhibitors of tim10 yeast	Cell	2941	1695
488912	Identify inhibitors of Sentrin-specific protease 8 (SENP8)	Biochemical	2491	3705
488915	Identify inhibitors of Sentrin-specific protease 6 (SENP6)	Biochemical	3568	2628
488917	Identify inhibitors of Sentrin-specific protease 7 (SENP7)	Biochemical	4283	1913
488918	Identify inhibitors of Sentrin-specific proteases (SENPs)	Biochemical	3691	2505
	using a Caspase-3 Selectivity assay			
492992	Idenfity inhibitors of the two-pore domain potassium	Cell	2094	2820
	channel (KCNK9)			
504607	Identify inhibitors of Mdm2/MdmX interaction	Cell	4830	1412
624504	Inhibitor hits of the mitochondrial permeability	Cell	3944	1090
	transition pore			
651739	Inihibition of Trypanosoma cruzi	Cell	4051	1324
651744	NIH/3T3 (mouse embryonic fibroblast) toxicity	Cell	3102	2306
652065	Identify molecules that bind r(CAG) RNA repeats	Cell	2966	1287

Table 1: List of assays from Pubchem that were used for this study

baseline methods.

3.1 Dataset Generation

We ran experiments on assay results deposited in PubChem (http://pubchem.ncbi.nlm. nih.gov/). We used 19 different assays, selected so at least several of them were closely related. Table 1 lists the assays that were used in our experiments. We included both cellular and biochemical assays and in some cases used multiple related assays, for example assays for different families of cytochrome P450 enzymes.

We generated molecular descriptors with Dragon³ to use as input to the various machine learning models. While Dragon can generate 4885 different descriptors, several of these descriptors were inapplicable to all of the compounds in our data sets. After excluding the inapplicable ones, we were left with 3764 molecular descriptors. Each descriptor was Z-score normalized over all the compounds in the union of all the assays. For some of the single task neural net models, we also generated additional binary features by thresholding other single descriptors. We selected descriptors and thresholds from decision nodes used in a boosted ensemble of limited depth decision trees.

³http://www.talete.mi.it/

3.2 QSAR Model Training

Using the assays, we treated the problem as a classification task using the active/inactive labels produced by the assay depositors. QSAR prediction can be formulated as a classification problem, a regression problem, or a ranking problem. All of our techniques are equally applicable to any of these problem formulations, but in this paper we only consider the binary classification version of the problem. A natural way to use a model that predicted activities would be to use it for virtual screening which is ultimately a ranking problem. Although the models we trained optimized classification performance, we use area under the ROC curve (AUC) as a performance metric since it emphasizes the ranking aspect of the problem more relevant to virtual screening applications.

For each assay, we held out at random 25% of the ligands to use as a test set, leaving the remaining 75% as a training set. We used several classifiers implemented in the scikitslearn [Pedregosa et al., 2011] package as baselines: random forests (RF), gradient boosted decision tree ensembles (GBM), and logistic regression (LR). We split the training set into four folds and trained each model four times with a different fold held out as validation data. We average the test set AUCs of the four models when reporting test set results. We used performance on the validation data to select the best particular model in each family of models. To the extent that the baseline models required metaparameter tuning (e.g. selecting the number of trees in the ensemble), we performed that tuning by hand using validation performance.

3.2.1 Neural Network Metaparameter Selection

Neural networks can have many important metaparameters, including architectural metaparameters, such as layer sizes and hidden unit link functions, optimization metaparameters, such as learning rates and momentum values, and regularization metaparameters such as the dropout probabilities for each layer, how long to train before stopping, and learning rate annealing schedules. We trained neural nets that used rectified linear units as well as neural nets that used sigmoidal units and most neural nets had between two and eight million parameters. In order to have an experimental protocol that avoids as many of the viccissitudes of human expert judgement as possible, we set all neural net metaparameters using Bayesian optimization [Snoek et al., 2012, 2013] of the validation AUC. Bayesian optimization is a type of sequential, model-based optimization ideally suited for globally optimizing blackbox, noisy functions while being parsimonious in the number of function evaluations. For metaparamter optimization, Bayesian optimization constructs a model of the function mapping metaparameter settings to validation AUC and suggests new jobs to run based on an acquisition function that balances exploration of areas of the space where the model is highly uncertainty with areas of the space likely to produce better results than the best job run so far. We used the Spearmint software that implements the Bayesian optimization algorithms from Snoek et al. [2012] and in particular we use the constrained version with warping enabled. See the appendix B for details of what neural net metaparameters we optimized over what ranges.

Bayesian optimization finds good model configurations very efficiently, but makes very strong use of the validation error and, with small validation sets, can quickly overfit the validation data. However, overfitting the validation data will only hurt the test set performance of the neural net models relative to the baselines that have fewer metaparameters that can be tuned readily and repeatably by hand.

4 Results and discussion

Table 2 contains our main results on all 19 assays we investigated. On 14 of the 19 assays, the best neural net achieves a test set AUC exceeding the best baseline result by a statistically signifigant margin. We measured statistical signifigance with t-tests using standard errors from training the models repeatedly on new bootstrap samples (see the appendix C for more details). On the remaining five assays there was no statistically signifigant difference between the best decesion tree ensemble baseline and the best neural net. On all assays, logistic regression was by far the worst performing model. On assays with closely related assays available, multi-task neural nets often performed better than their single-task counterparts, even with no a priori information on which particular assays were related to each other and despite having to make good predictions on all assays simultaneously, including unrelated ones.

The three assays (assay ids 1915, 2358, and 652065) that the decision tree baselines did best on relative to the neural net models (despite the differences not being statistically signifigant) had some of the fewest training cases and had no closely related assays in our dataset. Since we generally expect high-capacity, multi-task neural net models to provide benefits for larger datasets and when there are related assays to leverage, the three assays the baselines do comparitively better on are not surprising.

4.1 Multi-tasking vs combining assays

The 19 assays we used contain several groups of closely related assays. Specifically, we have five cytochrome P450 assays with minor variations, four assays for inhibition of Sentrinspecific proteases, and two related cellular assays for inhibition of particular yeast strains. When two assays are strongly *positively* correlated (which will happen when they are nearly identical and share enough compounds), simply merging the data from both might work as well as the more sophisticated multi-task neural net method that can leverage more general positive, negative, and feature-conditional correlations. In fact, if all the related assays we worked with were nearly identical, the gains we see from the multi-task neural net over the single-task methods might simply reflect the gains expected from adding more data to a single-task classifier. To investigate this issue, we created additional datasets that combined data from multiple assays. For example, the 488912 assay has three related

Assay	RF	GBM	NNET	MULTI
1851_1a2	0.915	0.926	0.926	0.938
1851_2c19	0.882	0.894	0.897	0.903
1851_2c9	0.876	0.891	0.889	0.907
1851_2d6	0.839	0.857	0.863	0.861
1851_3a4	0.871	0.896	0.895	0.897
1915	0.754	0.757	0.756	0.752
2358	0.745	0.764	0.738	0.751
463213	0.651	0.659	0.651	0.676
463215	0.614	0.610	0.613	0.654
488912	0.664	0.672	0.664	0.816
488915	0.700	0.713	0.723	0.873
488917	0.818	0.834	0.835	0.894
488918	0.785	0.800	0.784	0.842
492992	0.804	0.827	0.803	0.829
504607	0.673	0.670	0.684	0.670
624504	0.851	0.869	0.871	0.889
651739	0.775	0.793	0.790	0.825
651744	0.870	0.885	0.886	0.900
652065	0.787	0.793	0.793	0.792

Table 2: This table shows the average test set AUC for random forests (RF), gradient boosted decision tree ensembles (GBM), single-task neural nets (NNET), and multi-task neural nets (MULTI) on each assay. The multi-task neural nets are trained to make predictions for all assays at once. If the best neural net result on a particular assay is better than both decision tree baselines and the differences are statistically significant then we use boldface (the difference between the two nets may or may not be statistically significant). In the cases where the best decision tree baseline is better than both neural nets the differences are not statistically significant.

assays: 488915, 488917, and 488918. We added the training data from 488915, 488917, and 488918 to the 488912 training set while still testing on data exclusively from 488912. In this manner, we created 11 combined datasets and trained GBMs on them, since GBMs were the best performing non-neural net model.

Table 3 shows the results on these 11 datasets for single-task GBMs, multi-task neural nets using all 19 assays, and GBMs combining training data only from related assays. On 8 of the 11 datasets, the multi-task neural nets exhibit a statistically signifigant improvement over the single-task GBM and the combined training set GBM. On the remaining three datasets, there is not a statistically signifigant difference in performance between the best of the three models and the second best. Table 4 highlights results (also displayed in table 2) comparing single- and multi-task neural nets on assays with other related assays in our collection. On all but two of the 11 assays, the multi-task neural net trained using all 19 assays obtain statistically signifigant improvements in test AUC over the single-task neural nets. Since the multi-task neural net models can learn to ignore the other assays when making predictions for a particular assay, at worst they will only get somewhat weaker results than a single-task neural net because they waste capacity on irrelevant tasks. And, indeed, that is what we see in our results.

The 48891* series of assays are closely related enough for the GBMs trained on the combined training set of the four assays to do much better than the GBMs that use only the primary assay's training set. On some of the 48891* series assays, a GBM trained on the combined training sets even does better than a multi-task neural net trained to make predictions on all 19 datasets, although the improvement is not statistically signifigant. However, the multi-task neural net, in addition to having to make predictions for other unrelated assays, is not told that all of the 48891* series assays should be treated as the same problem. In contrast to the 48891* series, on the 1851_* series of assays, the GBMs trained on the combined 1851_* training sets do worse than the GBMs that just use the primary training set. On these assays, however, the multi-task neural net improves upon on both the single task GBM and neural net, showing that it can leverage information from the related assays in a more nuanced way. In practice we will often have somewhat related assays that are nevertheless far from identical and in this situation the multi-task neural net models can stil provide benefits, unlike a classifier simply combining the training sets from different assays.

On the 46321^{*} series of assays, although the GBMs on the combined training sets were better than the GBMs trained only on data from the primary assay, the multi-task neural net was better still. This result demonstrates that the two assays in the group are not sufficiently contradictory to confuse the GBM models on the combined training set (as happened with the 1851_* series), but there are still gains to be had from the multi-task neural net. The most interesting cases arise when assays are related but not positively correlated strongly enough to simply combine into a single dataset. In this scenario, multitask neural nets shine because they can use negative and partial correlations.

Primary Assay	GBM	MULTI	GBM Combined
1851_1a2	0.926	0.938	0.905
1851_2c19	0.894	0.903	0.883
1851_2c9	0.891	0.907	0.879
1851_2d6	0.857	0.861	0.840
1851_3a4	0.896	0.897	0.869
463213	0.659	0.676	0.665
463215	0.610	0.649	0.648
488912	0.672	0.825	0.815
488915	0.713	0.873	0.868
488917	0.834	0.915	0.909
488918	0.800	0.869	0.852

Table 3: Multi-task neural nets compare favorably to GBMs using training sets that combine related assays. Bold entries correspond to statistically signifigant differences.

Primary Assay	NNET	MULTI
1851_1a2	0.926	0.938
1851_2c19	0.897	0.903
1851_2c9	0.889	0.907
1851_2d6	0.863	0.861
1851_3a4	0.895	0.897
463213	0.651	0.676
463215	0.613	0.649
488912	0.664	0.825
488915	0.723	0.873
488917	0.835	0.915
488918	0.784	0.869

Table 4: For assays related to other assays in our collection, multi-task neural nets typically provide statistically signifigant improvements over single-task neural nets. Bold entries correspond to statistically signifigand differences.

4.2 Controlling overfitting without feature selection

Since we allowed Bayesian optimization to train fully connected neural networks with as many as about 3500 hidden units in a single layer, we used a variety of methods to prevent overfitting. Bayesian optimization quickly learned to enable dropout and use a non-zero L2 weight penalty. For any given assay, the best performing neural net always used some dropout and in preliminary hand-tuned experiments dropout seemed crucial as well.

Unlike a lot of QSAR work in the literature, for example Winkler [2002] who warns against including too many descriptors even if they contain relevant information, we do not advise performing feature selection to reduce the number of input dimensions drastically. Although not all the descriptors are necessary or very informative, well-regularized and properly trained neural networks can handle thousands of correlated input features. We trained neural nets using all (3764) descriptors as well as ones using the 2500, 2000, 1500, 1000, 500, or 100 most informative input features (as measured by information gain). On most assays, using the 2000-2500 most informative input descriptors did not degrage test set AUC very much, but using only 1500 or fewer typically produced a large an unnecessary drop in test set AUC. Figure 1 shows the test AUC for two representative assays. We generated the plot by training the best multi-task neural net using the relevant primary assay on different numbers of input descriptors.

4.3 Neural network depth

For the 19 assays we used and the descriptor set we used, changing the number of hidden layers had no consistent effect. We performed separate Bayesian optimization runs with one, two, and three hidden layer multi-task neural networks and one and two hidden layer single task neural networks. For single task neural nets, adding a second hidden layer had very little effect and the best result from each Bayesian optimization run for a particular model class achieved about the same test AUC regardless of the number of hidden layers. However, although there was no consistent trend for multi-task nets, allowing deeper models seemed to be occasionally important. Table 5 shows the results for the multi-task nets of different depths. Although the optimal depth is not the same or predictable across assays, on some assays there are large differences in performance between multi-task neural nets of different depths.

These depth results somewhat contradicts our experience in the Merck molecular activity prediction contest where we found using neural networks with more than one hidden layer to be crucial in almost all cases. Unfortunately, since neither the contest data nor the descriptors used in the contest are public or available for research and additional experiments, we can only speculate about the cause of this discrepancy. There were several assays in the contest with many more compounds than the assays we used from PubChem and larger datasets are more likely to provide enough training information to usefully fit additional hidden layers. Larger datasets affecting the optimal neural net depth is con-

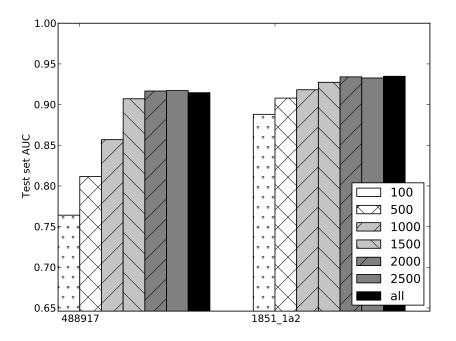


Figure 1: Test AUC on two representative assays of a multi-task neural net using different numbers of input features. For a given number of input descriptors, we selected the best features as measured by information gain.

Assay	1 hidden layer	2 hidden layers	3 hidden layers
1851_1a2	0.932	0.938	0.930
1851_2c19	0.903	0.884	0.881
1851_2c9	0.907	0.894	0.905
1851_2d6	0.855	0.861	0.768
1851_3a4	0.897	0.897	0.821
1915	0.752	0.754	0.740
2358	0.751	0.758	0.748
463213	0.676	0.678	0.672
463215	0.654	0.637	0.649
488912	0.768	0.816	0.825
488915	0.823	0.873	0.828
488917	0.886	0.894	0.917
488918	0.828	0.842	0.869
492992	0.829	0.827	0.826
504607	0.670	0.665	0.616
624504	0.889	0.881	0.893
651739	0.825	0.821	0.806
651744	0.895	0.900	0.894
652065	0.794	0.792	0.791

Table 5: Multi-task neural network results for neural nets with different numbers of hidden layers. We bolded the best result in a row when there was a statistically signifigant difference in test AUC between it and the second best entry in the row.

sistent with depth mattering more for the multi-task nets we trained since they use data from all the assays. The contest used the regression formulation of the task, unlike our experiments in this work that used the binary classification formulation, exaccerbating the difference in the number of bits of information in the training labels. Since we did not focus our efforts on trying many different descriptor sets, there may be types of descriptors Dragon does not compute that did exist in the contest data. A larger set of descriptors than the ones Dragon computes might improve our results. For example, the open source RDKit (www.rdkit.org) software provides Morgan fingerprint descriptors that the current version of Dragon does not compute and other commercial software packages such as MOE [2013.08] could have descriptor sets that add important information also.

5 Conclusions and future work

Our results demonstrate that neural networks using the latest techniques from the deep learning community can improve QSAR prediction accuracies and, in particular, there is a very natural and effective way of leveraging data from multiple assays when training a neural network QSAR model. However, many more experiments need to be done before we can settle on exactly the best way to solve QSAR problems with neural networks. Treating the task as a binary classification problem and using potentially unreliable active/inactive decisions from assay depositors in PubChem may not be the best way to approach the problem. In a virtual screening application, a notion of how active a compound is towards a particular target is essential and we plan to perform future work with the ranking version of the problem. Given the effectiveness of state-of-the-art Bayesian optimization software packages, practitioners should no longer fear the large number of metaparameters sophisticated neural network models can have since even with small datasets we were able to find very good metaparameter settings automatically. We also hope to develop better ways of implementing multi-task neural nets that can make use of additional information about which assays are likely to be related as well as target features and other side information. Given the rapid progress of research on neural network methods, we also hope to apply more advances from the deep learning community to QSAR problems.

Acknowledgements

We would like to acknowledge Christopher Jordan-Squire and Geoff Hinton for their work on our team during the Merck molecular activity challenge; without the contest we would not have started work on this project.

References

- Ajay, W. Patrick Walters, and Mark A. Murcko. Can we learn to distinguish between drug-like and nondrug-like molecules? *Journal of Medicinal Chemistry*, 41(18):3314– 3324, 1998. doi: 10.1021/jm970666c. URL http://pubs.acs.org/doi/abs/10.1021/ jm970666c.
- Frank R. Burden, Martyn G. Ford, David C. Whitley, and David A. Winkler. Use of automatic relevance determination in qsar studies using bayesian neural networks. *Journal of Chemical Information and Computer Sciences*, 40(6):1423–1430, 2000. doi: 10.1021/ci000450a. URL http://pubs.acs.org/doi/abs/10.1021/ci000450a.
- Frank R. and Burden. Robust qsar models using bayesian regularized neural networks. *Journal of Medicinal Chemistry*, 42(16):3183-3187, 1999. doi: 10.1021/jm980697n. URL http://pubs.acs.org/doi/abs/10.1021/jm980697n.
- 2013.08. Molecular Operating Environment (MOE). Chemical Computing Group Inc., 1010 Sherbooke St. West, Suite 910, Montreal, QC, Canada, H3A 2R7, 2013.

Ronan Collobert and Jason Weston. A Unified Architecture for Natural Language Processing: Deep Neural Networks with Multitask Learning. In *Proceedings of the 25th International Conference on Machine Learning (ICML-2008)*, pages 160–167, 2008.

James Devillers. Neural networks in QSAR and drug design. Academic Press, 1996.

- Hongying Du, Jie Wang, Zhide Hu, Xiaojun Yao, and Xiaoyun Zhang. Prediction of fungicidal activities of rice blast disease based on least-squares support vector machines and project pursuit regression. *Journal of Agricultural and Food Chemistry*, 56(22): 10785–10792, 2008. doi: 10.1021/jf8022194. URL http://pubs.acs.org/doi/abs/10. 1021/jf8022194.
- Dumitru Erhan, Pierre-Jean L'Heureux, Shi Yi Yue, and Yoshua Bengio. Collaborative filtering on a family of biological targets. J. Chem. Inf. Model., 46(2):626–635, 2006. URL http://dx.doi.org/10.1021/ci050367t.
- Dumitru Erhan, Aaron Courville, Yoshua Bengio, and Pascal Vincent. Why does unsupervised pre-training help deep learning? In *Proceedings of AISTATS 2010*, volume 9, pages 201–208, May 2010.
- Geoffrey E. Hinton, Simon Osindero, and Y. W. Teh. A fast learning algorithm for deep belief nets. *Neural Computation*, 18:1527–1554, 2006.
- Geoffrey E. Hinton, Li Deng, Dong Yu, George E. Dahl, Abdel-rahman Mohamed, Navdeep Jaitly, Andrew Senior, Vincent Vanhoucke, Patrick Nguyen, Tara N. Sainath, and Brian Kingsbury. Deep neural networks for acoustic modeling in speech recognition: The shared views of four research groups. *Signal Processing Magazine*, 29(6):82–97, 2012a.
- Geoffrey E. Hinton, Nitish Srivastava, Alex Krizhevsky, Ilya Sutskever, and Ruslan Salakhutdinov. Improving neural networks by preventing co-adaptation of feature detectors. *The Computing Research Repository (CoRR)*, abs/1207.0580, 2012b. URL http://arxiv.org/abs/1207.0580.
- Alex Krizhevsky, Ilya Sutskever, and Geoffrey E. Hinton. ImageNet classification with deep convolutional neural networks. In Peter L. Bartlett, Fernando C. N. Pereira, Christopher J. C. Burges, Lon Bottou, and Kilian Q. Weinberger, editors, Advances in Neural Information Processing Systems, pages 1106–1114, 2012.
- Peixun Liu and Wei Long. Current mathematical methods used in qsar/qspr studies. International Journal of Molecular Sciences, 10(5):1978–1998, 2009. ISSN 1422-0067. doi: 10.3390/ijms10051978. URL http://www.mdpi.com/1422-0067/10/5/1978.
- E.W. Lowe, M. Butkiewicz, N. Woetzel, and J. Meiler. Gpu-accelerated machine learning techniques enable qsar modeling of large hts data. In *Computational Intelligence in*

Bioinformatics and Computational Biology (CIBCB), 2012 IEEE Symposium on, pages 314–320, 2012.

- Eric Martin, Prasenjit Mukherjee, David Sullivan, and Johanna Jansen. Profile-qsar: a novel meta-qsar method that combines activities across the kinase family to accurately predict affinity, selectivity, and cellular activity. *Journal of chemical information and modeling*, 51(8):1942–1956, 2011.
- Olga Obrezanova, Gábor Csányi, Joelle MR Gola, and Matthew D Segall. Gaussian processes: a method for automatic qsar modeling of adme properties. *Journal of chemical information and modeling*, 47(5):1847–1857, 2007.
- F. Pedregosa, G. Varoquaux, A. Gramfort, V. Michel, B. Thirion, O. Grisel, M. Blondel, P. Prettenhofer, R. Weiss, V. Dubourg, J. Vanderplas, A. Passos, D. Cournapeau, M. Brucher, M. Perrot, and E. Duchesnay. Scikit-learn: Machine learning in Python. *Journal of Machine Learning Research*, 12:2825–2830, 2011.
- D. E. Rumelhart, G. E. Hinton, and R. J. Williams. Learning representations by backpropagating errors. *Nature*, 323(6088):533–536, 1986.
- Hongzong Si, Tao Wang, Kejun Zhang, Yun-Bo Duan, Shuping Yuan, Aiping Fu, and Zhide Hu. Quantitative structure activity relationship model for predicting the depletion percentage of skin allergic chemical substances of glutathione. Analytica Chimica Acta, 591(2):255 – 264, 2007.
- Jasper Snoek, Hugo Larochelle, and Ryan Prescott Adams. Practical bayesian optimization of machine learning algorithms. In Advances in Neural Information Processing Systems, pages 2960–2968, 2012.
- Jasper Snoek, Kevin Swersky, Richard Zemel, and Ryan Prescott Adams. Input warping for bayesian optimization of non-stationary functions. In Advances in Neural Information Processing Systems Workshop on Bayesian Optimization, 2013.
- Vladimir Svetnik, Andy Liaw, Christopher Tong, J. Christopher Culberson, Robert P. Sheridan, and Bradley P. Feuston. Random forest: A classification and regression tool for compound classification and qsar modeling. *Journal of Chemical Information and Computer Sciences*, 43(6):1947–1958, 2003.
- David A Winkler. The role of quantitative structure-activity relationships (qsar) in biomolecular discovery. *Briefings in bioinformatics*, 3(1):73–86, 2002.

A Stochastic gradient descent details

For all neural net training, we used minibatch stochastic gradient descent with momentum and backpropagation [Rumelhart et al., 1986] to compute the necessary gradients. Let Cbe the training objective function and let w be a generic neural net parameter. With $\langle \frac{\partial C}{\partial w} \rangle$ denoting the average objective function gradient over the current minibatch of cases, we used the following weight update formulas:

$$v(t) = \alpha v(t-1) + \epsilon \left(-\left\langle \frac{\partial C}{\partial w} \right\rangle - \lambda w \right)$$
$$w(t) = w(t-1) + v(t),$$

where ϵ is the learning rate or step size, α is the momentum strength, and λ is the weight cost strength.

B Bayesian optimization search space

We used the constrained version of Spearmint [Snoek et al., 2012] with warping enabled and labeled training runs that diverged as constraint violations. We let Spearmint optimize the metaparameters listed below with a budget of 30 (usually sequential) trials, although in a few preliminary experiments we used a 50 trial budget. The allowed ranges were decided based on our first single hidden layer, single-task neural net Spearmint run and in some cases slightly adjusted for other Spearmint runs. In general, since the adjustments were not major ones, it is safe to pick the largest range we ever used for any given metaparameter; at worst a few extra jobs would be required.

Metaparameters:

- dropout fractions $\in [0, 0.75]$, with a separate metaparameter for the input layer and each hidden layer
- the number of training epochs in [2, 100] for nets with a single hidden layer and in [2, 120] for nets with two or more hidden layers
- the number of hidden units in each layer (allowed to be different in different layers)

For single task neural nets, no hidden layer was allowed more than 3072 units. The minimum number of hidden units in a layer for a single task neural net was 16 in our first single hidden layer run and 64 all other times. For multi-task neural nets we had a minimum of 512 units in each hidden layer and allowed up to 3584 units, except for the three hidden layer models which we constrained to a maximum of 2048.

• the annealing delay fraction $\in [0, 1]$, or in other words the fraction of the training iterations that must complete before we start annealing the learning rate

We used a continuous parameterization of the fraction even though the training program would end up rounding when computing what epoch to start annealing the learning rate.

• the initial learning rate

The learning rate is applied to the average gradient over a minibatch. We allowed initial learning rates in $\in [0.001, 0.25]$ for all multi-task neural net experiments and our initial single-task, single hidden layer Spearmint run. All other single-task neural net experiments allowed Spearmint to select an initial learning rate in $\in [0.001, 0.3]$.

• the type of annealing, either exponential or linear

The annealing mode was a discrete choice. For linear annealing, the plot of learning rate versus epoch is a straight, downward sloping line intersecting the initial learning rate when annealing starts and the final learning rate when training stops. Linear annealing used a final learning rate of 10^{-8} . Once annealing has started, exponential annealing multiplies the learning rate by a constant shrinkage factor each iteration with the factor chosen to ensure that the learning rate when training stops is the final learning rate. Exponential annealing used a final learning rate of 10^{-6} . We do not believe the precise value matters very much as long as it is small.

- momentum $\in [0, 0.95]$
- the L^2 weight cost $\in [0, 0.005]$ except for single-task neural nets with two hidden layers in which case we allowed weight costs in [0, 0.007]
- the hidden unit activation function, either logistic sigmoids or rectified linear units For simplicity, we forced all hidden units in a network to use the same activation function.
- scale (standard deviation) of the initial random weights $\in [0.01, 0.2]$

We used Gaussian initial random weights. All weight matrices used the same scale except for the weights from the inputs to the first hidden layer which the subsequent metaparameter controls.

• natural log of the multiplier for the scale of the bottom (input to hidden) weight matrix $\in [-1, 1]$

We allowed Spearmint to set the scale of the lowest weight matrix as a multiplicative adjustment to the scale of the rest of the weights. In this way, Bayesian optimization can set the bottom weight matrix to have a scale up to e times smaller or larger than the other weight matrices.

C Statistical signifigance determination

Since we presented tables of results for 19 different assays and the assays have different numbers of data cases in them, it is important to have at least some simple notion of what differences in test AUC between models on a single assay are stronger or weaker evidence of a true difference in performance. The simple bootstrap procedure outlined below allowed us to indicated which differences between model families were large enough to be potentially interesting in a way that took into account the variability of our results due to the particular training sample and the inherent variabilities of model training.

In order to get standard errors for the signifigance tests we mentioned in the main text, we used bootstrap sampling. We trained on 8 different bootstrap samples of the complete training set. Let y_1 and y_2 be the average test set AUCs of two different models after normal (not bootstrap samples) training on the different training folds. Let σ_1^2 and σ_2^2 be the unbiased sample variances corresponding to the test AUC results of the two models after training on the new training sets that were sampled from the original training set with replacement. We called a difference between table entries y_1 and y_2 statistically signifigant when

$$|y_1 - y_2| > 1.96\sqrt{\frac{\sigma_1^2 + \sigma_2^2}{8}}.$$

Although using the difference of cross validation mean test AUCs $y_1 - y_2$ on the left hand side in the test instead of the difference in mean test AUC across the relevant bootstrap training runs is non-standard, since the data sets we used are small, only training on bootstrap samples noticeably degrades performance since a bootstrap sample often will not contain all possible training cases. Our approximate test rejects many seemingly large test AUC differences as insignificant statistically on the assays with very little data (e.g. 2358 and 1915) which is reasonable behavior given the variability of model test AUCs on datasets that are that small.

In our comparisons that involved GBMs using the combined training sets from multiple assays, we did not recompute new standard errors and instead used the single task GBM standard errors. Avoiding this computation may overestimate the uncertainty in the test AUCs of the GBMs using the combined training sets since training the same model with more data generally reduces the training sample variance. Overestimating the uncertainty in the test AUCs of the GBMs trained on the combined data would only give them an advantage when compared to the neural net models since the multi-task neural nets compared to them had better results.